



Geophysical Research Letters°

RESEARCH LETTER

10.1029/2021GL096960

Key Points:

- Coincident reductions in seismic wavespeeds and lower-crustal reflectivity occur from south-to-north along the Hikurangi forearc
- Legacy seismic reflection data attribute the forearc transition to along-strike differences in the updip extent of the Torlesse Backstop
- Shallow slow-slip is focused updip of the backstop, suggesting it may impact the location of shallow frictional transitions at Hikurangi

Supporting Information:

Supporting Information may be found in the online version of this article.

Correspondence to:

D. Bassett, d.bassett@gns.cri.nz

Citation:

Bassett, D., Arnulf, A., Henrys, S., Barker, D., van Avendonk, H., Bangs, N., et al. (2022). Crustal structure of the Hikurangi margin from SHIRE seismic data and the relationship between forearc structure and shallow megathrust slip behavior. *Geophysical Research Letters*, 49, e2021GL096960. https://doi.org/10.1029/2021GL096960

Received 8 NOV 2021 Accepted 3 JAN 2022

© 2022 The Authors.

This is an open access article under the terms of the Creative Commons Attribution-NonCommercial License, which permits use, distribution and reproduction in any medium, provided the original work is properly cited and is not used for commercial purposes.

Crustal Structure of the Hikurangi Margin From SHIRE Seismic Data and the Relationship Between Forearc Structure and Shallow Megathrust Slip Behavior

Dan Bassett¹, Adrien Arnulf², Stuart Henrys¹, Dan Barker¹, Harm van Avendonk², Nathan Bangs², Shuichi Kodaira³, Hannu Seebeck¹, Laura Wallace^{1,2}, Andrew Gase², Thomas Luckie⁴, Katie Jacobs¹, Brook Tozer¹, Ryuta Arai³, David Okaya⁴, Kimi Mochizuki⁵, Gou Fujie³, and Yojiro Yamamoto³

¹GNS Science, Lower Hutt, New Zealand, ²Institute for Geophysics, Jackson School of Geosciences, University of Texas at Austin, Austin, TX, USA, ³Japan Agency for Marine-Earth Science and Technology, Yokohama, Japan, ⁴University of Southern California, Los Angeles, CA, USA, ⁵Earthquake Research Institute (ERI), University of Tokyo, Tokyo, Japan

Abstract Marine multichannel and wide-angle seismic data constrain crustal structure along a 530 km margin-parallel transect of the Hikurangi subduction zone. The subducting Hikurangi Plateau crust (V_P 5.0–7.4 km/s) is ~1 km thicker (11 ± 1 km) and mantle velocities are ~0.2 km/s higher (V_P 8.3–8.5 km/s) beneath south/central Hikurangi relative to north Hikurangi. In the overthrusting plate, an abrupt 0.5 km/s south-to-north reduction in forearc wavespeeds occurs in concert with a change in seismic reflection character. We analyze legacy seismic data to show that the forearc transition likely reflects lateral variability in the updip extent of the Torlesse Backstop. Furthermore, we map this unit along-strike and note a broad correlation between the backstop and down-dip extent of shallow slow-slip. We propose that the geological architecture of the overthrusting plate contributes to spatial variability in the location of shallow frictional transitions along the Hikurangi margin, impacting both seismic and tsunami hazard.

Plain Language Summary Some subduction zones produce the largest earthquakes and tsunami on Earth, while others slip freely. To understand what factors impact subduction zone slip behavior, we analyze seismic data along a 530 km long transect spanning a transition from strong (south Hikurangi) to weak (central/north Hikurangi) interseismic locking. From south-to-north, we find that seismic wavespeeds in the overthrusting plate undergo an abrupt (~10%) reduction, which coincides with a reduction in seismic reflectivity. We show that these changes likely reflect differences in the offshore (updip) extent of basement rocks within the forearc crust, which we map using seismic data. These maps also show that the offshore extent of basement rocks is broadly correlated with the maximum depth of shallow slow-slip events. We propose that geological architecture of the overthrusting plate may contribute to spatial variability in megathrust slip-behavior, impacting both seismic and tsunami hazard along the Hikurangi margin.

1. Introduction

The seismogenic (earthquake generating) portion of subduction megathrusts is flanked by regions of stable (aseismic) or conditionally stable fault slip behavior (Lay et al., 2012). The location of these transitions imposes key constraints on tsunami generation, the proximity of strong ground shaking to densely populated coastal communities, and the area, and thus magnitude, of earthquakes rupturing the seismogenic zone. Although frictional transitions are often attributed to thermal, metamorphic or diagenetic processes (Hyndman & Wang, 1993; Moore & Saffer, 2001; Oleskevich et al., 1999), depth dependent variations in the frequency-content, source duration and slip amplitude of earthquakes (Bilek & Lay, 1999; Lay et al., 2012) have recently been linked to variations in rigidity of the overthrusting plate (Sallarès & Ranero, 2019). Overthrusting plate structure played a key role in modulating the distribution of slip in the 2011 Mw 9.0 Tohoku-oki earthquake (Bassett et al., 2016), but there are also many examples of great earthquakes being stalled (Robinson et al., 2006), deflected (Kodaira et al., 2000) or stopped (Bilek, 2010) by subducting topographic relief. Ultimately, both factors are clearly important and at many subduction zones it is not agreed what properties cause some megathrust segments to lock up and accumulate large quantities of elastic strain, while adjacent segments slip with relative ease.

BASSETT ET AL. 1 of 11

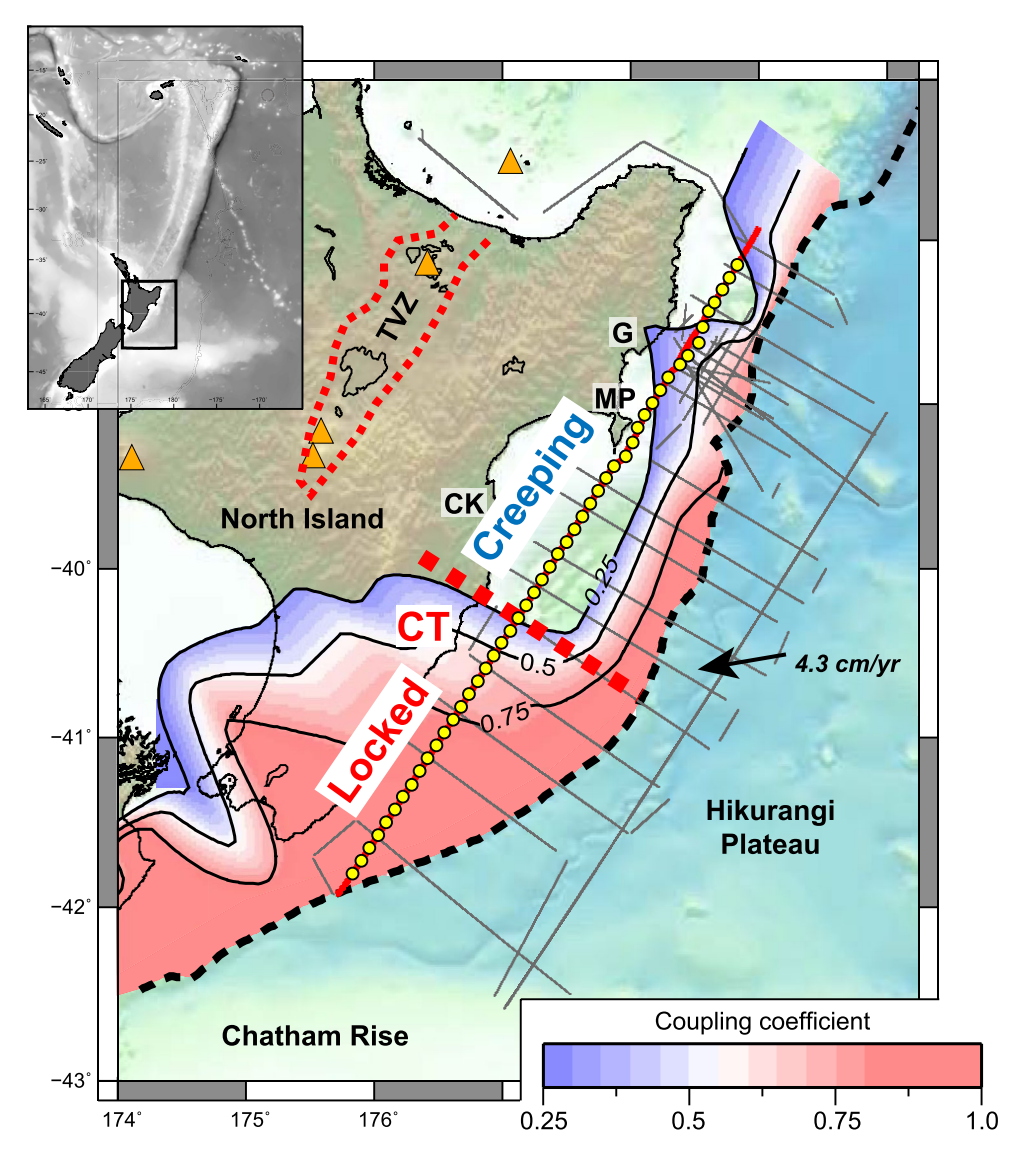


Figure 1. Tectonic setting and geophysical data. (a) Hikurangi subduction zone, New Zealand. Gray lines show marine seismic profiles collected during The Seismogenesis at Hikurangi Integrated Research Experiment (SHIRE). The forearc transect is marked in red with Ocean Bottom Seismometers in yellow. Color shows interseismic coupling (Wallace, Barnes, et al., 2012). Orange Triangles mark active volcanoes. Annotation: CT = Cape Turnagain, CK = Cape Kidnappers, MP = Mahia Peninsula, G = Gisborne, TVZ = Taupo Volcanic Zone.

One of the best expressed along-strike transitions in megathrust slip behavior occurs along the Hikurangi margin, New Zealand (Figure 1). In south Hikurangi, onshore geodetic data show the megathrust to be strongly locked to \sim 30 km depth and reveal a band of deep (25–40 km), long-duration (1–2 years), slow-slip events (SSEs) that likely mark the down-dip frictional transition zone (Wallace, Beavan, et al., 2012). The north Hikurangi megathrust, by contrast, is characterized by weak interseismic coupling, frequent, shallow (2–15 km) short duration (<1 month) SSEs and produced two tsunami earthquakes in 1947 (Doser & Webb, 2003; Wallace, Beavan, et al., 2012; Wallace et al., 2016).

A wide range of physical properties may contribute to the spatial variability in slip behavior along the Hikurangi megathrust. Controlled and natural source seismic observations show the overthrusting plate in the region of strong geodetic locking to be characterized by higher V_P , lower V_P/V_S ratio and lower attenuation, and have been interpreted to indicate higher effective stress levels, lower porosity and/or a lower volume of fluids in the overthrusting plate (Bassett et al., 2014; Eberhart-Phillips & Bannister, 2015; Eberhart-Phillips et al., 2017; Henrys

BASSETT ET AL. 2 of 11



et al., 2020; Reyners & Eberhart-Phillips, 2009). The tectonic stress state flips from extension to transpression across the coupling transition, influencing both structural permeability in the overthrusting plate and the depth of the frictional to viscous transition along the subduction megathrust (Barnes et al., 2019; Fagereng & Ellis, 2009; Wallace, Fagereng, & Ellis, 2012). On the subducting plate, incoming sediment thickness thins from >4 km offshore Wairarapa to ~1 km offshore Gisborne and the lithologic, mechanical and frictional heterogeneity associated with the subduction of rougher crust has been proposed to play a key role in facilitating shallow slow slip and creep along the north Hikurangi megathrust (Barker et al., 2018; Barnes et al., 2020; Chesley et al., 2021; Wallace et al., 2009; Wang & Bilek, 2014). In this study, we analyze new marine geophysical data spanning the full length of the Hikurangi subduction zone to constrain crustal architecture along-strike and possible linkages with spatial variability in megathrust slip behavior.

2. Marine Geophysical Data

2.1. Data Acquisition

We analyze wide-angle and multichannel seismic (MCS) data acquired along 530 km of the Hikurangi forearc during The Seismogenesis at Hikurangi Integrated Research Experiment (SHIRE; Bangs & Shipboard-Scientific-Party, 2018; Barker et al., 2019). Wide-angle seismic data were recorded by 49 Ocean Bottom Seismometers (OBSs) deployed at \sim 10 km intervals by R/V *Tangaroa*. These OBSs are multi-component JAMSTEC instruments including a triaxial, short-period seismograph (4.5 Hz natural frequency) and a hydrophone. OBSs recorded seismic energy from 9,492 airgun shots from a tuned 36 air-gun array with a total volume of 108 L (6,600 inch³), which was charged to 13.1 MPa (1,900 \pm 100 Psi) and towed at 9 m depth by the R/V *Marcus G Langseth*. Airgun shots were spaced at \sim 50 m for the southwestern 440 km and \sim 150 m between model km 440–530. Coincident MCS data were recorded by a 12.8 km long, 1,008 channel hydrophone streamer towed at 10 m depth with an 18 s record length and 2 ms sample rate.

2.2. Wide-Angle Seismic Data and Tomography

Wide-angle data were processed using a minimum-phase Butterworth frequency filter (2–20 Hz), before trace amplitude balancing and coherency filtering (Figures 2a and 2b and S4 in Supporting Information S1). From OBS gathers, we identified phases associated with refractions through the crust of the Australian forearc and subducting Hikurangi Plateau (P_g), reflections from the base (Moho) of the subducting Hikurangi Plateau crust (P_mP), and refractions through the underlying mantle (P_n). Picking errors were visually estimated and range from 50 to 200 ms, with a mean error of 97 ms. Travel-time picks were sampled at 250 m in the shot-domain and the total number of picks for P_g , P_mP , and P_n phases are 23,344, 5,396, and 10,854, respectively.

Ray-coverage at shallow depth was improved by including streamer refractions identified in MCS shot-gathers. We interpreted every 10th shot-gather (i.e., 500 m shot-spacing) and down-sampled first-arrivals to 250 m in the receiver-domain. Collectively, we incorporated 22,060 streamer refractions with offsets ranging from 2.1 to 12.8 km (mean 7.9 km) and picking errors visually estimated between 50 and 100 ms.

Travel-time tomography was carried out using a version of the algorithm originally developed by Van Avendonk et al. (2004), which has been fully parallelized and optimized for large computational problems (Arnulf et al., 2018). This algorithm uses the shortest-path method (Moser, 1991) for the forward calculation of synthetic travel-times. Weighted travel-time residuals are then back-propagated along ray-paths, with iterative model updates calculated by a minimizing a least squares cost-function penalizing the misfit between observed and calculated travel-times and model roughness. To account for the crooked-line geometry, raytracing was performed in a 540×10 km mesh extending down to 50 km depth, discretized at 1 km intervals horizontally and 250 m vertically.

We have applied a Monte Carlo approach performing 100 tomographic inversions. Our starting models consist of a series of simple 1D velocity models hanging below the seabed. Across these models, velocities at a given depth in the crust and mantle vary by up-to 1 km/s and 0.5 km/s respectively. The Moho of the subducting Hikurangi Plateau is randomly prescribed a starting depth 10, 12, or 14 km below the subduction interface (Williams et al., 2013). To prevent vertical smearing of travel-time misfits, each tomographic model was constructed by first inverting P_g arrivals recorded by OBSs, before subsequently incorporating deeper penetrating P_mP , and P_n

BASSETT ET AL. 3 of 11



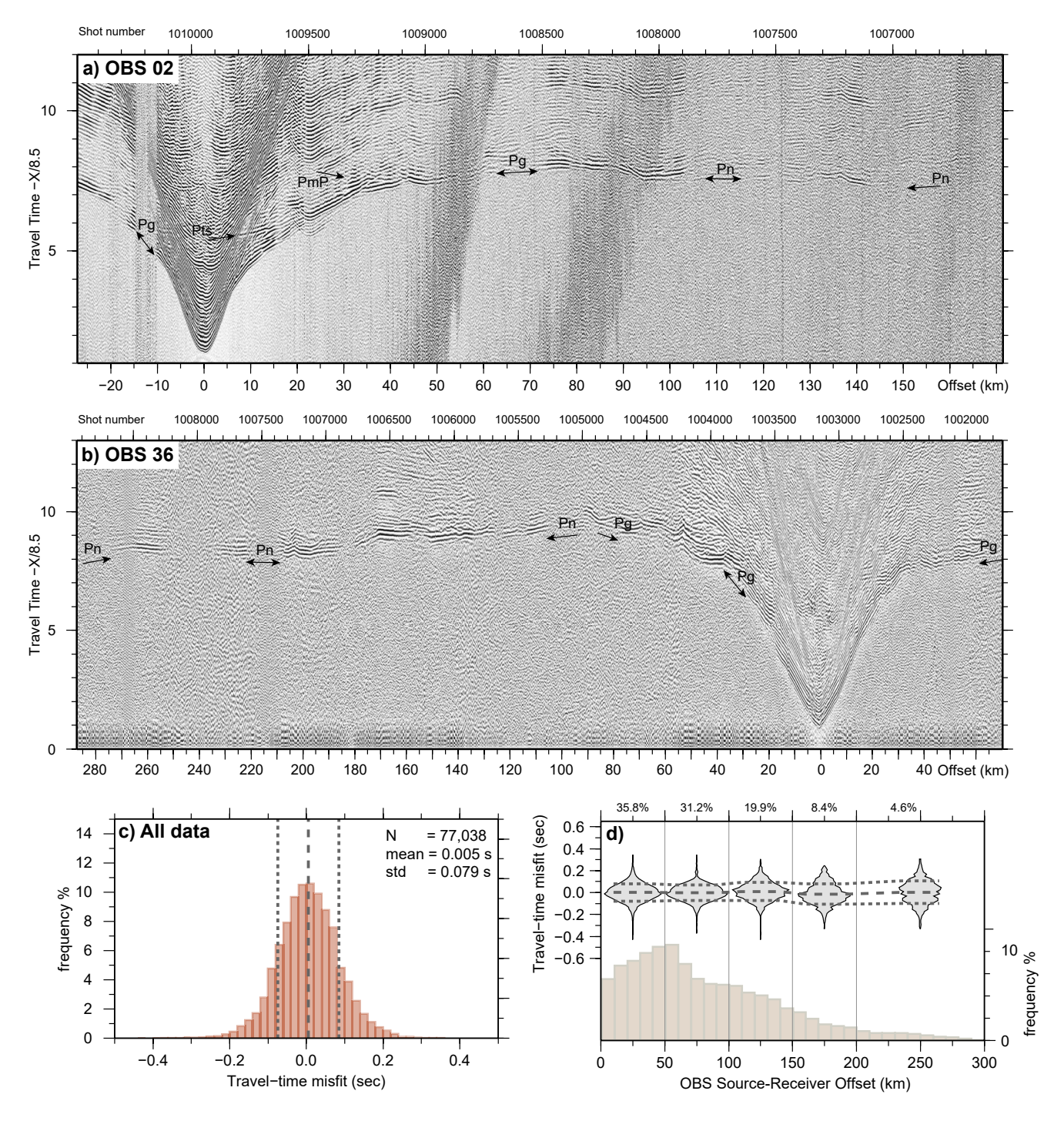


Figure 2. Wide-angle data and misfit statistics. (a) Wide-angle seismic data recorded at OBS02 and (b) OBS36. Seismic data are reduced to 8.5 km/s with labels indicating phase interpretations. (c) Histogram showing the distribution of travel-time misfit for our final velocity model. (d) Violin plots of the travel-time misfit distribution for Ocean Bottom Seismometer data within source-receiver offset bins. The underlying histogram shows the source-receiver offset distribution with labels indicating the proportion of data within each bin.

phases. Picks from marine streamer data were incorporated last to avoid introducing bias associated with their higher density. The final, average, velocity model has a Chi-square misfit χ^2 of 1.02 and a root mean squared (RMS) error of 81 ms (Figures 2c and 2d).

BASSETT ET AL. 4 of 11



Spatial resolution was assessed by preforming checkerboard tests and by calculating the standard deviation of velocities and interface depths across 100 velocity models. The results of these tests are provided in Supporting Information.

2.3. Multichannel Seismic Data Processing

SHIRE seismic reflection data were processed using a shipboard pre-stack processing sequence consisting of resampling to 4 ms, band-limited swell noise suppression (0–3 Hz), velocity analysis and spherical divergence gain adjustment. MCS shot-gathers were sorted into 6.25 m CMP bins (126–168 nominal fold), before Kirchhoff Poststack 2D migration with stacking velocities. Post-stack migration processing included Butterworth band-pass frequency filtering (5–85 Hz) and gain adjustment (1 s gate).

3. Results: Forearc Wavespeeds Vary in Concert With Geodetic Locking

Figure 3b shows *P*-wave seismic velocity (V_P) along the SHIRE forearc transect. The upper-crust of the subducting Hikurangi Plateau is 5–6 km thick with wavespeeds increasing from 5.5–7.0 km/s. A shallower velocity gradient is maintained through the lower-crust with wavespeeds typically \leq 7.3 km/s, but locally \geq 7.4 km/s. The crustal thickness of the Hikurangi Plateau is 11 ± 1 km south of model km 350, which is \sim 1 km thicker than the crustal thickness observed (10 ± 1 km) further north. This contrast in crustal structure is consistent with results obtained along margin-normal wide-angle seismic profiles traversing the Hikurangi Plateau in South and North Hikurangi respectively (Gase et al., 2021; Mochizuki et al., 2019).

Below the Moho, wavespeeds in the subducting mantle also exhibit along-strike variability and differ by \sim 0.2 km/s north and south of model km \sim 350. To the north, V_P is typically 8.1–8.2 km/s at the Moho and does not exceed 8.3 km/s within the area of ray-coverage. V_P south of model km 350, by contrast, is regionally \geq 8.3 km/s and is \sim 8.5 km/s below the central portion of the transect. These mantle wavespeeds are also consistent with those measured in the margin-normal direction by intersecting active-source profiles in North (7.8–8.1 km/s; Gase et al., 2021) and South (8.3 \pm 0.25 km/s; Mochizuki et al., 2019) Hikurangi, respectively. Our results in South Hikurangi are slightly slower than observations indicating high mantle velocities (8.8 \pm 0.2 km/s) made both along-strike (Galea, 1992; Kayal & Smith, 1984), and more recently down-dip (Herath et al., 2020; Stern et al., 2020). This difference may reflect the turning-depths of raypaths (<30 km) analyzed in our study being 5–20 km shallower than most observations from which higher wavespeeds are determined.

Above the megathrust, we resolve a sharp along-strike transition in crustal structure of the overthrusting forearc (Figures 3b and 3c). Along the southern Hikurangi forearc, Neogene sediment cover ($V_P \le 3.0$ km/s) is <2 km thick, V_P exceeds 4.0 km/s within 4 km of the seabed and 4–5 km of crust overlying the megathrust has $V_P \ge 4.5$ km/s (red in Figure 3a). In north Hikurangi, sedimentary cover is ~1 km thicker (~3 km), V_P is typically <4.0 km/s within 7 km of the seabed and lower-crustal velocities are ~0.5 km/s slower than those observed at equivalent depths in south Hikurangi.

The contrast in forearc wavespeeds is further illustrated by calculating the average (1-D) V_p -depth profile along our transect (black in Figure 3d) and plotting our velocity model as the deviation from this average (Figure 3c). This calculation highlights the location, magnitude, and regional extent of the contrast in forearc wavespeeds, and is supported by local V_p -depth profiles calculated along the southern and central/northern Hikurangi margin, which differ by 0.4–0.7 km/s at depths 3–10 km below the seafloor (Figure 3e). These V_p -depth profiles calculated offshore are analogous to those derived from onshore-offshore seismic records by Bassett et al. (2014). A comparison between these profiles reveals a striking similarity between 1-D profiles for North Hikurangi and shows that onshore-offshore data require higher wavespeeds at crustal depths (>3 km b.s.f) in South Hikurangi (Figure 3d). This comparison suggests low forearc wavespeeds are maintained near and down-dip of the coast in North Hikurangi and the north-south contrast in forearc wavespeeds becomes even more pronounced inboard of the SHIRE forearc transect.

Figure 3a shows slip deficit rate on the subduction megathrust derived from onshore geodetic data (Wallace, Barnes, et al., 2012). This comparison shows the transition in forearc structure to be well correlated with the base of the ramp in slip-rate deficit that marks the transition from a creeping megathrust in the north to an interseismically locked megathrust in the south.

BASSETT ET AL. 5 of 11



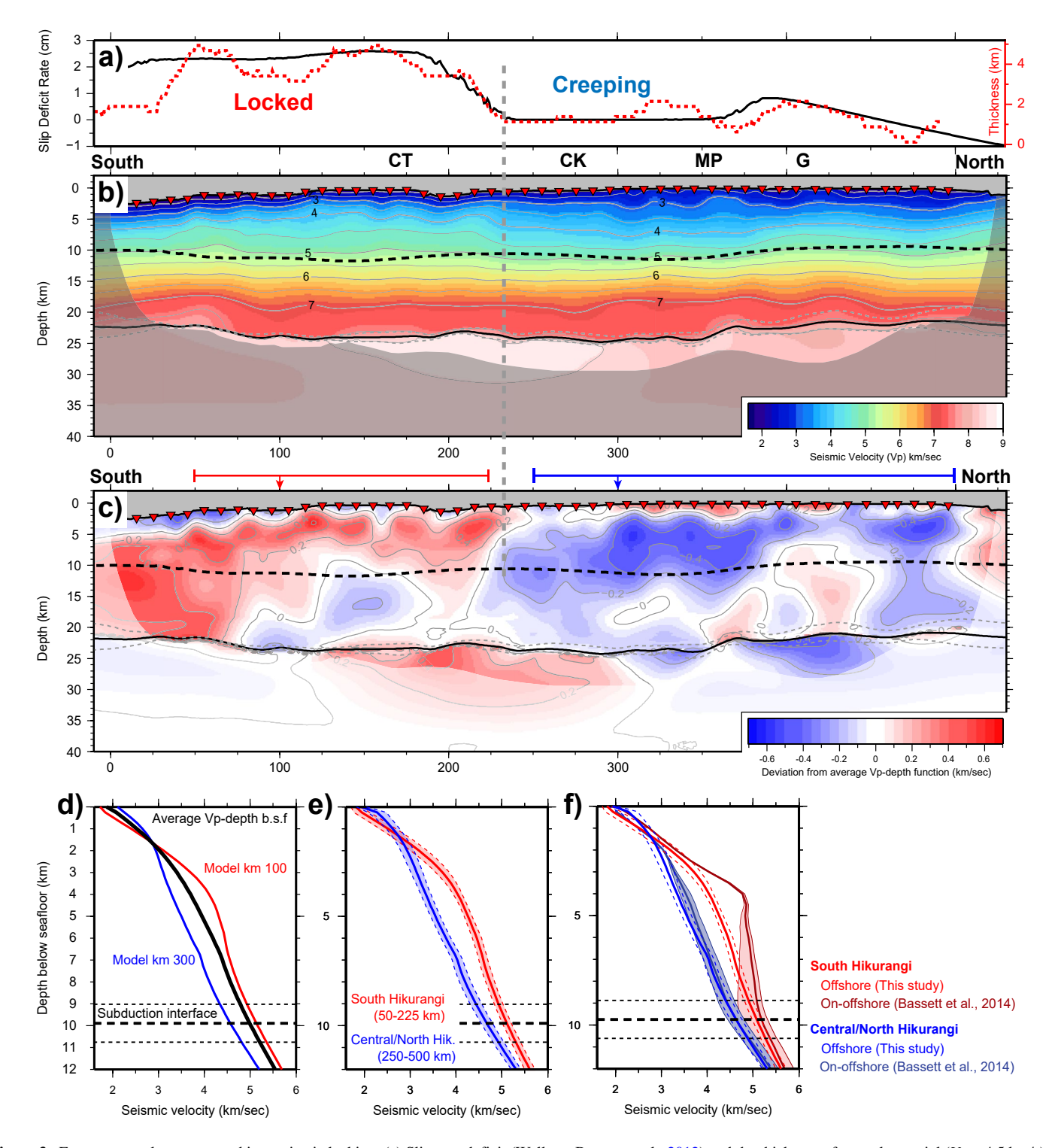


Figure 3. Forearc crustal structure and interseismic locking. (a) Slip-rate deficit (Wallace, Barnes, et al., 2012) and the thickness of crustal material ($V_P \ge 4.5 \text{ km/s}$) overlying the subduction interface. (b) P-wave (V_P) seismic velocity along the Seismogenesis at Hikurangi Integrated Research Experiment (SHIRE) forearc transect. The subduction interface (Williams et al., 2013) and base of the subducting plate are marked by dashed and solid black lines respectively. Vertical dashed gray line marks concomitant reductions in seismic velocity and slip-rate deficit. (c) Deviation from the average velocity-depth profile along the SHIRE forearc transect. (d) Regional 1-D V_P -depth profile. Dashed horizontal and dotted black lines show the mean depth and standard deviation of the subduction interface. (e) Local V_P -depth profiles for South (red) and North (blue) Hikurangi respectively. The dashed envelope represents one standard deviation. (f) Comparison between offshore (this study) and onshore-offshore (Bassett et al., 2014) 1-D V_P -depth profiles. Annotation: CT = Cape Turnagain, CK = Cape Kidnappers, MP = Mahia Peninsula, G = Gisborne.

BASSETT ET AL. 6 of 11

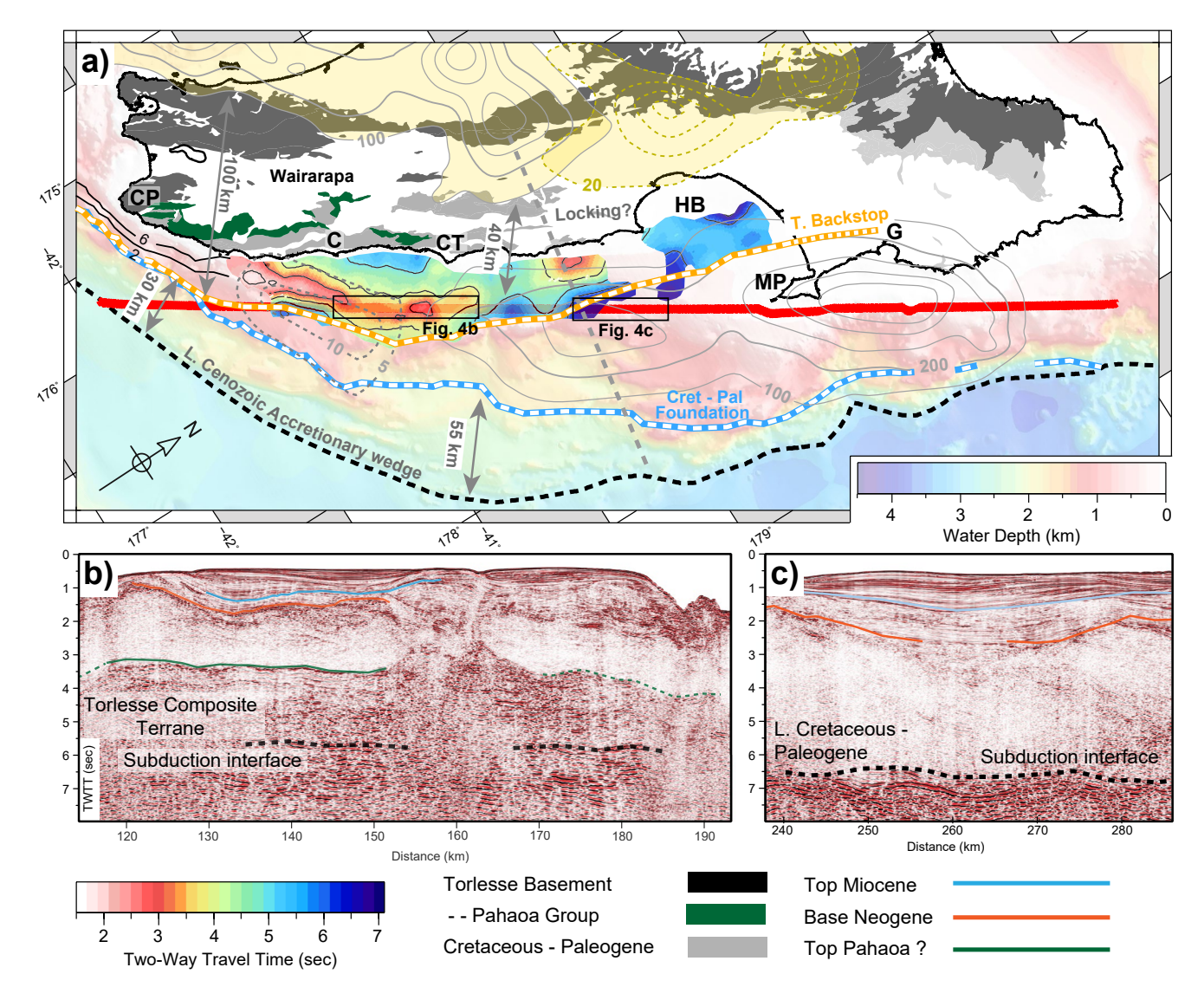


Figure 4. Forearc geology at Hikurangi. (a) Onshore geology, offshore morphology and (b) seismic reflection character of the Hikurangi forearc south and (c) north of the transition in forearc wavespeeds. The contoured grid offshore shows the 3D geometry (two-way time) of the mid-crustal reflector used to map the offshore distribution of the Torlesse Composite Terrane. The dashed orange and blue lines mark the updip extent of Torlesse Composite Terrane, and the boundary between Late Cretaceous-Paleogene passive margin foundation and the Late Cenozoic frontal accretionary wedge (Barnes et al., 2010; Gase et al., 2021). Solid and dashed gray contours show cumulative shallow slow-slip (2002–2014) and a smaller slow-slip event (SSE) offshore Wairarapa (Wallace, 2020; Wallace, Beavan, et al., 2012). Solid and dashed yellow contours show cumulative deep slow-slip and a smaller SSE beneath the Kaimanawa ranges. Gray arrows highlight along-strike variations in width of the Late Cenozoic accretionary wedge and the zone of frictional locking. Annotation: CP = Cape Palliser, C = Castlepoint, CT = Cape Turnagain, HB = Hawke Bay, MP = Mahia Peninsula, G = Gisborne.

3.1. Seismic Reflection Image and Physical Interpretation of Along-Strike Variation in Wavespeeds

Seismic velocity is controlled by elastic moduli and density and is strongly impacted, via porosity, by effective stress. The wavespeed variations recorded along the Hikurangi forearc (Figure 3) may therefore reflect differences in effective stress levels and/or pore-fluid pressure (Bassett et al., 2014), upper-plate stress-state (Fagereng & Ellis, 2009; Townend et al., 2012; Wallace, Fagereng, & Ellis, 2012), the spatial distribution of geological terranes (Reyners & Eberhart-Phillips, 2009), or the formation of low wavespeed, high-porosity damage zones created by subducting relief (Sun et al., 2020), which has been geophysically imaged in North Hikurangi (Arai et al., 2020; Barker et al., 2018; Chesley et al., 2021).

A key observation revealed by SHIRE MCS data is that the seismic reflection character of the forearc crust varies in concert with forearc wavespeeds (Figure 4). In south Hikurangi, the lower crust of the upper plate is highly

BASSETT ET AL. 7 of 11



reflective and capped by a high-amplitude, laterally contiguous mid-crustal reflector (Figure 4b). North of the wavespeed transition, by contrast, the lower-crust is acoustically transparent (Figure 4c).

High lower-crustal reflectivity in the south Hikurangi forearc has been interpreted to indicate the presence of Early Cretaceous (110–100 Ma) Pahaoa Group rocks of the Torlesse Composite Terrane (Barker et al., 2009; Mountjoy & Barnes, 2011) overlying the plate interface. The Torlesse Composite Terrane constitutes geological basement in eastern North Island, and Pahaoa Group rocks outcrop in the coastal foothills of Wairarapa, less than 30 km from our offshore seismic transect (Heron et al., 2015; Mortimer, 2004). To obtain regional constraints on the subsurface distribution of this unit, we have mapped the capping mid-crustal reflector through an extensive database of legacy seismic reflection data (Figure S4 in Supporting Information S1). Two-way travel-time to the top of this unit is shown in Figure 4a, and the shallowing of this reflector toward Pahaoa outcrops onshore (dark green in Figure 4a) further supports existing lithologic interpretations (Mountjoy & Barnes, 2011; Plaza-Faverola et al., 2016). The updip extent of this unit is marked by the orange dash and the location where this updip limit intersects our 2D profile is well correlated with the reduction in forearc wavespeeds (dashed gray line in Figure 4a). We therefore suggest that coincident reductions in seismic velocity and lower-crustal reflectivity simply mark where Torlesse Basement no longer extends far enough updip to be imaged along our 2D profile.

This interpretation is supported by along-strike differences in the proximity of Torlesse Basement outcrops to the SHIRE forearc transect (Figure 4a). In south Hikurangi, Torlesse Basement outcrops at Cape Palliser (Pahau Terrain) and in the coastal foothills of Wairarapa (Pahaoa Group), less than 30 km from our offshore profile (Barnes & Korsch, 1990; Begg et al., 2000; Lee et al., 2002). From south-to-north, these units are progressively overlain by a younger or stratigraphically higher succession of Late Cretaceous to Paleogene "cover" and passive margin sequences (Field & Uruski, 1997; Lee et al., 2002). This pattern is consistent with the northward deepening of the reflector we associate with the top of the Torlesse Composite terrain. North of Hawke Bay, Torlesse outcrops are restricted to the axial ranges and western Raukumara Peninsula (Mazengarb & Speden, 2000). These outcrops are >50 km further from the SHIRE forearc transect than their counterparts along the Wairarapa coast and it is possible their subsurface extent does not extend far enough updip (~80 km) to be imaged along our offshore profile.

Higher wavespeeds within Torlesse Basement likely reflect the higher degree of induration associated with accretion to the Gondwana forearc, relative to the Late Cretaceous-Paleogene "cover" or passive margin rocks that occupy the forearc updip and along-strike (Barnes et al., 2010; Bland et al., 2015; Moore & Speden, 1984; Mortimer, 2004). It is possible a contribution to the wavespeed contrast is made by the stress regime in the upper-plate changing from extension (north) to transpression (south) south of Hawkes Bay (Dimitrova et al., 2016; Townend et al., 2012). The mid-crustal reflector and concomitant variation in lower crustal reflection character, however, is less likely to be caused by changes in stress state and we therefore retain along-strike variability in the distribution of geological terrains as a key component of our interpretation.

4. Discussion

The south-to-north reduction in forearc wavespeeds along the SHIRE forearc transect is consistent with earlier results from onshore-offshore travel-times (Bassett et al., 2014), earthquake tomography (Eberhart-Phillips et al., 2017), and explanations linking ultra-long (>450 s) durations of long-period ground motions after the 2016 M7.8 Kaikoura earthquake to the reverberation of seismic waves within a low-velocity wedge (Kaneko et al., 2019). In addition to the hazard to infrastructure posed by long-duration, long-period ground shaking, this "basin effect" leads to prolonged dynamic stressing on the plate interface and may have promoted the dynamic-triggering of slow slip by the Kaikoura earthquake (Wallace et al., 2017, 2018).

Building on the work of Barnes et al. (2010), our mapping allows rocks overlying the Hikurangi megathrust to be subdivided in map view into a Torlesse Backstop (Orange dash), overlying Late Cretaceous and Paleogene passive margin foundation rocks (Blue dash), and the Late Cenozoic accretionary wedge (Figure 4a). The gray contours show that the cumulative distribution of shallow slow slip (2002–2014) and a smaller (dashed) SSE offshore Wairarapa (Wallace, 2020; Wallace, Beavan, et al., 2012) are both focused updip of the backstop and in regions where Late Cretaceous and Paleogene passive margin foundation rocks overly the subduction interface. This relationship suggests the geological architecture of the overthrusting plate may play a role in modulating the updip extent of unstable (Torlesse Backstop) and conditionally stable (passive margin foundation) fault slip at Hikurangi. This link may be due to a contrast in induration or frictional properties (Moore & Speden, 1984),

BASSETT ET AL. 8 of 11



the influence of different material properties on structural permeability and the ability of the wedge to maintain or relieve excess fluid pressure (Reyners & Eberhart-Phillips, 2009), and/or the strength and stress-state of the wedge and the mechanics by which it accumulates and releases elastic strain. It is also consistent with observations from other subduction zones linking margin-normal changes in the consolidation or lithification of the upper-plate with shallow transitions in megathrust slip behavior (Byrne et al., 1988; Nakanishi et al., 2002; Sallarès & Ranero, 2019; Watt & Brothers, 2021). The key point is that the location of frictional transitions (as defined by the down-dip extent of shallow slow slip) appears to be more spatially variable than that defined by thermal and diagenetic models (Hyndman et al., 1995; Moore & Saffer, 2001; Oleskevich et al., 1999). This conclusion has implications for the characterization of earthquake and tsunami hazard along the Hikurangi margin.

The updip extent of co-seismic slip is a key control on tsunami excitation. Where the outer-forearc is narrow, earthquake rupture occurs at shallower depth, beneath deeper water, and has a higher likelihood of reaching the trench (Hu & Wang, 2008). Each of these factors enhance tsunami generation. The implication at Hikurangi is to imply a higher tsunami hazard and likelihood of trench-breaking rupture offshore southernmost Hikurangi, where the position of the Torlesse Backstop may extend frictional locking to within 30 km from the deformation front (Figure 4a). This distance is comparable to the ~30 km width of the outer-wedge where the 2011 M9 Tohoku-oki earthquake maintained large co-seismic slip amplitudes to the NE Japan trench (Miura et al., 2005). Tsunami hazard in south Hikurangi may be further compounded if the stress shadow from the deeper locked patch results in high slip-deficit rates being maintained updip of the Torlesse Backstop, despite the reduction in frictional strength implied by the occurrence of shallow slow slip (Lindsey et al., 2021). In this case, the increased width of the outer-wedge between Castlepoint and Cape Turnagain (~55 km) may be significant in limiting the updip extent of co-seismic slip offshore Wairarapa (Hu & Wang, 2008).

The final implication concerns how the position of the Torlesse Backstop impacts the location and spatial extent of frictional locking. In Hikurangi, the landward migration of Torlesse Basement rocks, coupled with the northward increase in slab dip (Williams et al., 2013), causes the updip transition to shift westward and progressively deepen from ~11 km offshore and south of Cape Turnagain, to ~14 km at Hawke Bay and >16 km north of Mahia Peninsula (Figure 4a). What is key is that across Cape Turnagain, slip transients marking the down-dip transition also impinge on the seismogenic zone, with SSEs beneath Manawatu occurring nearer the trench and at shallower depth (<20-25 km) relative to the adjacent deeply locked region (Wallace, Beavan et al., 2012). Combined, these changes abruptly reduce the distance separating shallow and deep regions of transient slip from 80-100 km in south Hikurangi, to a narrow, 40 km wide transitional corridor north of Cape Turnagain (Figure 4), where large magnitude (Mw ≥ 7) earthquakes occurred in 1904, 1958 and 1993 and inferences of locking are supported by observations of contractional strain (Haines & Wallace, 2020; Wallace, 2020). This reduction in the area of frictional locking will locally reduce the amount of elastic strain transmitted to the overthrusting plate (Wallace, Beavan et al., 2012). It may also increase slip-rate on the shallow megathrust by reducing the magnitude of the stress-shadow cast updip (Lindsey et al., 2021). This latter effect may contribute to along-strike differences in the amount of shallow slow-slip and raises the possibility of a distinct reduction in megathrust shear stressing rate south of Cape Turnagain.

Acknowledgments

This study was supported by U.S National Science Foundation Grants: 1658010, 1657480 and 1615815, by the New Zealand Ministry of Business Innovation and Employment (MBIE) Endeavour Grant: Diagnosing peril posed by the Hikurangi subduction zone, and by public research funding from the MBIE Science Investment Fund to GNS Science. We thank the Editor Lucy Flesch, and Anne Trehu and Frauke Klingelhoefer for helpful reviews that improved the manuscript. We thank the Captain and crew of the R/V M.G. Langseth (MGL1708) and R/V Tangaroa (TAN1710). We also thank MBIE and the Tangaroa Reference Group for its support in granting ship time for TAN1710. Seismic processing and interpretation were conducted using GLOBE Claritas and Seisware. Figures were constructed using the Generic Mapping Tools (Wessel et al., 2019; Wessel & Smith, 1991).

Data Availability Statement

Raw marine multi-channel seismic (MCS) data used in this study are available through the Lamont Academic Seismic Portal (http://www.marine-geo.org/collections/). The processed MCS section is available through the GNS Science Database Catalogue (http://dx.doi.org/10.21420/TQ67-8F60). Ocean Bottom Seismograph data are available through the JAMSTEC Seismic Survey Database (http://www.jamstec.go.jp/obsmcs_db/e/survey/data_area.html?cruise=TAN1710).

References

Arai, R., Kodaira, S., Henrys, S., Bangs, N., Obana, K., Fujie, G., et al. (2020). Three-Dimensional P wave velocity structure of the northern Hikurangi margin from the NZ3D experiment: Evidence for fault-bound anisotropy. *Journal of Geophysical Research: Solid Earth*, 125(12), e2020JB020433. https://doi.org/10.1029/2020jb020433

Arnulf, A., Harding, A., Kent, G., & Wilcock, W. (2018). Structure, seismicity, and accretionary processes at the hot spot-influenced Axial Seamount on the Juan de Fuca Ridge. *Journal of Geophysical Research: Solid Earth*, 123(6), 4618–4646. https://doi.org/10.1029/2017jb015131
 Bangs, N., & Shipboard-Scientific-Party. (2018). SHIRE project cruise report Seismogenesis at Hikurangi integrated research experiment (Vol. 89). University of Texas Institute of Geophysics.

BASSETT ET AL. 9 of 11



- Barker, D. H. N., Henrys, S., Caratori Tontini, F., Barnes, P. M., Bassett, D., Todd, E., & Wallace, L. (2018). Geophysical constraints on the relationship between seamount subduction, slow slip, and tremor at the north Hikurangi subduction zone, New Zealand. Geophysical Research Letters, 45(23), 12804–12813. https://doi.org/10.1029/2018gl080259
- Barker, D. H. N., Sutherland, R., Henrys, S., & Bannister, S. (2009). Geometry of the Hikurangi subduction thrust and upper plate, North Island, New Zealand. *Geochemistry, Geophysics, Geosystems*, 10. https://doi.org/10.1029/2008gc002153
- Barker, D. H. N., Van Avendonk, H., Fujie, G., & Science, G. (2019). Seismogenesis at Hikurangi integrated research experiment (SHIRE) report of RV Tangaroa Cruise TAN1710, 23 Oct 20-Nov 2017: GNS Science report.
- Barnes, J. D., Cullen, J., Barker, S., Agostini, S., Penniston-Dorland, S., Lassiter, J. C., et al. (2019). The role of the upper plate in controlling fluid-mobile element (Cl, Li, B) cycling through subduction zones: Hikurangi forearc, New Zealand. *Geosphere*, 15(3), 642–658. https://doi.org/10.1130/ges02057.1
- Barnes, P. M., & Korsch, R. J. (1990). Structural analysis of a middle Cretaceous accretionary wedge, Wairarapa, New Zealand. New Zealand Journal of Geology and Geophysics, 33(2), 355–375. https://doi.org/10.1080/00288306.1990.10425693
- Barnes, P. M., Lamarche, G., Bialas, J., Henrys, S., Pecher, I., Netzeband, G. L., et al. (2010). Tectonic and geological framework for gas hydrates and cold seeps on the Hikurangi subduction margin. *New Zealand: Marine Geology*, 272(1), 26–48. https://doi.org/10.1016/j.margeo.2009.03.012
- Barnes, P. M., Wallace, L. M., Saffer, D. M., Bell, R. E., Underwood, M. B., Fagereng, A., et al. (2020). Slow slip source characterized by lithological and geometric heterogeneity. *Science Advances*, 6(13), eaay3314. https://doi.org/10.1126/sciadv.aay3314
- Bassett, D., Sandwell, D. T., Fialko, Y., & Watts, A. B. (2016). Upper-plate controls on co-seismic slip in the 2011 magnitude 9.0 Tohoku-oki earthquake. *Nature*, 531(7592), 92–96. https://doi.org/10.1038/nature16945
- Bassett, D., Sutherland, R., & Henrys, S. (2014). Slow wavespeeds and fluid overpressure in a region of shallow geodetic locking and slow slip, Hikurangi subduction margin. New Zealand: Earth and Planetary Science Letters, 389, 1–13. https://doi.org/10.1016/j.epsl.2013.12.021 Begg, J. G., Johnston, M. R., & McSaveney, E. (2000). Geology of the Wellington area.
- Bilek, S. L. (2010). Invited review paper: Seismicity along the South American subduction zone: Review of large earthquakes, tsunamis, and subduction zone complexity. *Tectonophysics*, 495(1), 2–14. https://doi.org/10.1016/j.tecto.2009.02.037
- Bilek, S. L., & Lay, T. (1999). Rigidity variations with depth along interplate megathrust faults in subduction zones. *Nature*, 400(6743), 443–446. https://doi.org/10.1038/22739
- Bland, K. J., Uruski, C. I., & Isaac, M. J. (2015). Pegasus basin, eastern New Zealand: A stratigraphic record of subsidence and subduction, ancient and modern. New Zealand Journal of Geology and Geophysics, 58(4), 319–343. https://doi.org/10.1080/00288306.2015.1076862
- Byrne, D. E., Davis, D. M., & Sykes, L. R. (1988). Loci and maximum size of thrust earthquakes and the mechanics of the shallow region of subduction zones. *Tectonics*, 7, 833–857. https://doi.org/10.1029/tc007i004p00833
- Chesley, C., Naif, S., Key, K., & Bassett, D. (2021). Fluid-rich subducting topography generates anomalous forearc porosity. *Nature*, 595(7866), 255–260. https://doi.org/10.1038/s41586-021-03619-8
- Dimitrova, L., Wallace, L., Haines, A., & Williams, C. (2016). High-resolution view of active tectonic deformation along the Hikurangi subduction margin and the Taupo Volcanic Zone, New Zealand. New Zealand Journal of Geology and Geophysics, 59(1), 43–57. https://doi.org/10.1080/00288306.2015.1127823
- Doser, D. I., & Webb, T. H. (2003). Source parameters of large historical (1917–1961) earthquakes, North Island, New Zealand. Geophysical Journal International, 152(3), 795–832. https://doi.org/10.1046/j.1365-246x.2003.01895.x
- Eberhart-Phillips, D., & Bannister, S. (2015). 3-D imaging of the northern Hikurangi subduction zone, New Zealand: Variations in subducted sediment, slab fluids and slow slip. *Geophysical Journal International*, 201(2), 838–855. https://doi.org/10.1093/gji/ggv057
- Eberhart-Phillips, D., Bannister, S., & Reyners, M. (2017). Deciphering the 3-D distribution of fluid along the shallow Hikurangi subduction zone using P-and S-wave attenuation. *Geophysical Journal International*, 211(2), 1032–1045. https://doi.org/10.1093/gji/ggx348
- Fagereng, A., & Ellis, S. (2009). On factors controlling the depth of interseismic coupling on the Hikurangi subduction interface. New Zealand: Earth and Planetary Science Letters, 278(1–2), 120–130. https://doi.org/10.1016/j.epsl.2008.11.033
- Field, B. D., & Uruski, C. I. (1997). Cretaceous-Cenozoic geology and petroleum systems of the East Coast Region (p. 301). Institute of Geological and Nuclear Sciences Limited, Institute of Geological and Nuclear Sciences Monograph.
- Galea, P. (1992). Observations of very high P-velocities in the subducted slab, New Zealand, and their relation with the slab geometry. *Geophysical Journal International*, 110(2), 238–250.
- Gase, A. C., Bangs, N., & Van Avendonk, H. J. (2021). Crustal structure of the northern Hikurangi margin, New Zealand: Variable accretion and upper plate strength influenced by rough subduction. *Journal of Geophysical Research B: Solid Earth.*
- Haines, A. J., & Wallace, L. M. (2020). New Zealand-wide geodetic strain rates using a physics-based approach. *Geophysical Research Letters*, 47(1), e2019GL084606. https://doi.org/10.1029/2019gl084606
- Henrys, S., Eberhart-Phillips, D., Bassett, D., Sutherland, R., Okaya, D., Savage, M., et al. (2020). Upper plate heterogeneity along the southern Hikurangi margin, New Zealand. *Geophysical Research Letters*, 47(4), e2019GL085511. https://doi.org/10.1029/2019gl085511
- Herath, P., Stern, T. A., Savage, M. K., Bassett, D., Henrys, S., & Boulton, C. (2020). Hydration of the crust and upper mantle of the Hikurangi Plateau as it subducts at the southern Hikurangi margin. *Earth and Planetary Science Letters*, 541, 116271. https://doi.org/10.1016/j.epsl.2020.116271
- Heron, D. W., Edbrooke, S., Forsyth, P., & Jongens, R. (2015). Geological map of New Zealand, 1: 1,000,000. Institute of Geological and Nuclear Sciences Limited.
- Hu, Y., & Wang, K. (2008). Coseismic strengthening of the shallow portion of the subduction fault and its effects on wedge taper. *Journal of Geophysical Research*, 113, B12. https://doi.org/10.1029/2008jb005724
- Hyndman, R., & Wang, K. (1993). Thermal constraints on the zone of major thrust earthquake failure: The Cascadia subduction zone. *Journal of Geophysical Research*, 98(B2), 2039–2060. https://doi.org/10.1029/92jb02279
- Hyndman, R., Wang, K., & Yamano, M. (1995). Thermal constraints on the seismogenic portion of the southwestern Japan subduction thrust. Journal of Geophysical Research, 100, 15373–15392. https://doi.org/10.1029/95jb00153
- Kaneko, Y., Ito, Y., Chow, B., Wallace, L. M., Tape, C., Grapenthin, R., et al. (2019). Ultra-long duration of seismic ground motion arising from a thick, low-Velocity sedimentary wedge. *Journal of Geophysical Research: Solid Earth*, 124(10), 10347–10359. https://doi.org/10.1029/2019jb017795
- Kayal, J., & Smith, E. G. (1984). Upper mantle P-wave velocities in the southeast North Island, New Zealand. Tectonophysics, 104(1-2), 115–125. https://doi.org/10.1016/0040-1951(84)90105-7
- Kodaira, S., Takahashi, N., Nakanishi, A., Miura, S., & Kaneda, Y. (2000). Subducted seamount imaged in the rupture zone of the 1946 Nankaido earthquake. Science, 289(5476), 104–106. https://doi.org/10.1126/science.289.5476.104

BASSETT ET AL. 10 of 11



- Lay, T., Kanamori, H., Ammon, C. J., Koper, K. D., Hutko, A. R., Ye, L., et al. (2012). Depth-varying rupture properties of subduction zone megathrust faults. *Journal of Geophysical Research*, 117(B4). https://doi.org/10.1029/2011jb009133
- Lee, J. M., Begg, J., & Forsyth, P. (2002). Geology of the Wairarapa area. Institute of Geological & Nuclear Sciences.
- Lindsey, E. O., Mallick, R., Hubbard, J. A., Bradley, K. E., Almeida, R. V., Moore, J. D., et al. (2021). Slip rate deficit and earthquake potential on shallow megathrusts. *Nature Geoscience*, 14(5), 321–326. https://doi.org/10.1038/s41561-021-00736-x
- Mazengarb, C., & Speden, I. G. (2000). *Geology of the Raukumara area* (p. 60). Lower Hutt Institute of Geological and Nuclear Sciences Limited, Institute of Geological and Nuclear Sciences 1:250,000 geological map.
- Miura, S., Takahashi, N., Nakanishi, A., Tsuru, T., Kodaira, S., & Kaneda, Y. (2005). Structural characteristics off Miyagi forearc region, the Japan Trench seismogenic zone, deduced from a wide-angle reflection and refraction study. *Tectonophysics*, 407(3), 165–188. https://doi. org/10.1016/j.tecto.2005.08.001
- Mochizuki, K., Sutherland, R., Henrys, S., Bassett, D., Van Avendonk, H., Arai, R., et al. (2019). Recycling of depleted continental mantle by subduction and plumes at the Hikurangi Plateau large igneous province, southwestern Pacific Ocean. Geology, 47(8), 795–798. https://doi.org/10.1130/g46250.1
- Moore, J. C., & Saffer, D. (2001). Updip limit of the seismogenic zone beneath the accretionary prism of southwest Japan: An effect of diagenetic to low-grade metamorphic processes and increasing effective stress. *Geology*, 29(2), 183–186. https://doi.org/10.1130/0091-7613(2001)029 <0183:ulotsz>2.0.co;2
- Moore, P. R., & Speden, I. G. (1984). The early Cretaceous (Albian) sequence of eastern Wairarapa.
- $Mortimer, N. (2004). \ New \ Zealand's \ geological foundations. \ \textit{Gondwana Research}, 7, 261-272. \ https://doi.org/10.1016/s1342-937x(05)70324-5 \ Moser, T. (1991). \ Shortest \ path \ calculation \ of \ seismic \ rays. \ \textit{Geophysics}, 56(1), 59-67. \ https://doi.org/10.1190/1.1442958$
- Mountjoy, J. J., & Barnes, P. M. (2011). Active upper plate thrust faulting in regions of low plate interface coupling, repeated slow slip events, and coastal uplift: Example from the Hikurangi Margin, New Zealand. *Geochemistry, Geophysics, Geosystems*, 12. https://doi.org/10.1029/2010gc003326
- Nakanishi, A., Kodaira, S., Park, J.-O., & Kaneda, Y. (2002). Deformable backstop as seaward end of coseismic slip in the Nankai Trough seismogenic zone. Earth and Planetary Science Letters, 203(1), 255–263. https://doi.org/10.1016/s0012-821x(02)00866-x
- Oleskevich, D., Hyndman, R., & Wang, K. (1999). The updip and downdip limits to great subduction earthquakes: Thermal and structural models of Cascadia, south Alaska, SW Japan, and Chile. *Journal of Geophysical Research*, 104(B7), 14965–14991. https://doi.org/10.1029/1999jb900060
- Plaza-Faverola, A., Henrys, S., Pecher, I., Wallace, L., & Klaeschen, D. (2016). Splay fault branching from the Hikurangi subduction shear zone: Implications for slow slip and fluid flow. Geochemistry, Geophysics, Geosystems, 17(12), 5009–5023.
- Reyners, M., & Eberhart-Phillips, D. (2009). Small earthquakes provide insight into plate coupling and fluid distribution in the Hikurangi subduction zone, New Zealand. Earth and Planetary Science Letters, 282(1), 299–305. https://doi.org/10.1016/j.epsl.2009.03.034
- Robinson, D. P., Das, S., & Watts, A. B. (2006). Earthquake rupture stalled by a subducting fracture zone. Science, 312(5777), 1203–1205. https://doi.org/10.1126/science.1125771
- Sallarès, V., & Ranero, C. R. (2019). Upper-plate rigidity determines depth-varying rupture behaviour of megathrust earthquakes. *Nature*, 576(7785), 96–101.
- Stern, T., Lamb, S., Moore, J. D., Okaya, D., & Hochmuth, K. (2020). High mantle seismic P-wave speeds as a signature for gravitational spreading of superplumes. Science Advances, 6(22), eaba7118. https://doi.org/10.1126/sciadv.aba7118
- Sun, T., Saffer, D., & Ellis, S. (2020). Mechanical and hydrological effects of seamount subduction on megathrust stress and slip. *Nature Geoscience*, 13(3), 249–255, https://doi.org/10.1038/s41561-020-0542-0
- Townend, J., Sherburn, S., Arnold, R., Boese, C., & Woods, L. (2012). Three-dimensional variations in present-day tectonic stress along the Australia–Pacific plate boundary in New Zealand. Earth and Planetary Science Letters, 353, 47–59. https://doi.org/10.1016/j.epsl.2012.08.003
- Van Avendonk, H. J., Shillington, D. J., Holbrook, W. S., & Hornbach, M. J. (2004). Inferring crustal structure in the Aleutian island arc from a sparse wide-angle seismic data set. *Geochemistry, Geophysics, Geosystems*, 5. https://doi.org/10.1029/2003gc000664
- Wallace, L. M. (2020). Slow slip events in New Zealand. Annual Review of Earth and Planetary Sciences, 48. https://doi.org/10.1146/annurev-earth-071719-055104
- Wallace, L. M., Barnes, P., Beavan, J., Van Dissen, R., Litchfield, N., Mountjoy, J., et al. (2012). The kinematics of a transition from subduction to strike-slip: An example from the central New Zealand plate boundary. *Journal of Geophysical Research*, 117. https://doi.org/10.1029/2011jb008640
- Wallace, L. M., Beavan, J., Bannister, S., & Williams, C. (2012). Simultaneous long-term and short-term slow slip events at the Hikurangi subduction margin, New Zealand: Implications for processes that control slow slip event occurrence, duration, and migration. *Journal of Geophysical Research*, 117, B11. https://doi.org/10.1029/2012jb009489
- Wallace, L. M., Fagereng, Å., & Ellis, S. (2012). Upper plate tectonic stress state may influence interseismic coupling on subduction megathrusts. *Geology*, 40(10), 895–898. https://doi.org/10.1130/g33373.1
- Wallace, L. M., Hreinsdottir, S., Ellis, S., Hamling, I., D'Anastasio, E., & Denys, P. (2018). Triggered slow slip and afterslip on the southern Hikurangi subduction zone following the Kaikōura earthquake. *Geophysical Research Letters*. https://doi.org/10.1002/2018g1077385
- Wallace, L. M., Kaneko, Y., Hreinsdóttir, S., Hamling, I., Peng, Z., Bartlow, N., et al. (2017). Large-scale dynamic triggering of shallow slow slip enhanced by overlying sedimentary wedge. Nature Geoscience, 10(10), 765–770. https://doi.org/10.1038/ngeo3021
- Wallace, L. M., Reyners, M., Cochran, U., Bannister, S., Barnes, P. M., Berryman, K., et al. (2009). Characterizing the seismogenic zone of a major plate boundary subduction thrust: Hikurangi Margin, New Zealand. *Geochemistry, Geophysics, Geosystems*, 10. https://doi.org/10.1029/2009gc002610
- Wallace, L. M., Webb, S. C., Ito, Y., Mochizuki, K., Hino, R., Henrys, S., et al. (2016). Slow slip near the trench at the Hikurangi subduction zone, New Zealand. Science, 352(6286), 701–704. https://doi.org/10.1126/science.aaf2349
- Wang, K., & Bilek, S. L. (2014). Invited review paper: Fault creep caused by subduction of rough seafloor relief. *Tectonophysics*, 610, 1–24. https://doi.org/10.1016/j.tecto.2013.11.024
- Watt, J. T., & Brothers, D. S. (2021). Systematic characterization of morphotectonic variability along the Cascadia convergent margin: Implications for shallow megathrust behavior and tsunami hazards. Geosphere, 17(1), 95–117. https://doi.org/10.1130/ges02178.1
- Wessel, P., Luis, J., Uieda, L., Scharroo, R., Wobbe, F., Smith, W., & Tian, D. (2019). The generic mapping tools version 6. Geochemistry, Geophysics, Geosystems, 20(11), 5556–5564. https://doi.org/10.1029/2019gc008515
- Wessel, P., & Smith, W. H. (1991). Free software helps map and display data: Eos. *Transactions American Geophysical Union*, 72(41), 441–446. https://doi.org/10.1029/90e000319
- Williams, C. A., Eberhart-Phillips, D., Bannister, S., Barker, D. H., Henrys, S., Reyners, M., & Sutherland, R. (2013). Revised interface geometry for the Hikurangi subduction zone, New Zealand. Seismological Research Letters, 84(6), 1066–1073. https://doi.org/10.1785/0220130035

BASSETT ET AL. 11 of 11